Robust Superhydrophobic Foam: A Graphdiyne-Based Hierarchical Architecture for Oil/Water Separation

Xin Gao, Jingyuan Zhou, Ran Du, Ziqian Xie, Shibin Deng, Rong Liu, Zhongfan Liu, and Jin Zhang**

Exploitation and design of functionalized materials with superhydrophobicity have stimulated many interests owing to their intriguing potential applications, ranging from self-cleaning,[1,2] antifogging,[3–5] oil/water separation,[6–8] and even energy-related applications.[9] Inspired by nature (e.g., lotus leaves,[10] enormous artificial superhydrophobic materials have been designed and fabricated by combining rough surface structures and low-surface-energy coatings.[11,12] Of all these, 3D porous architectures were believed to be beneficial for prolonging working life and enhancing separation efficiency in the field of oil/water separation, for their intrinsic microlevel porous structures, and longer size along the *z*-direction than 2D substrates.[13] Although several methods have been utilized to fabricate superhydrophobic 3D porous architectures, including bottom-up type (e.g., sol–gel methods,[14,15] chemical vapor deposition[16,17] and top-down type (e.g., modification of as-obtained polymer foams[18–20] or metal foams,[21,22] most products such as graphene-based foams and modified sponges are fragile or unable to withstand abrasion. More importantly, without effective control means, few methods could generate ordered microstructures on 3D porous substrates, which brings great difficulties in predicting the wettability and thus designing desirable superhydrophobic materials. Therefore, fabricating ordered microstructures on mechanically robust 3D porous substrates is of great importance.

Graphdiyne, as a new member of carbon family, has aroused many interests due to its extraordinary physical and chemical properties. Its unique sp–sp^2 carbon atoms, uniform pores, and highly π-conjugated structure result in numerous applications including Li storage,[23,24] hole-transporting materials,[25] catalysis,[26–28] and field emission devices.[29,30] Previously, it was found that the morphology of graphdiyne can be readily controlled on 2D copper foils.[30] Inspired by this, we hypothesize that if the ordered microstructures based on graphdiyne could be transferred to the 3D porous foams, great superhydrophobic materials can be fabricated for both practical applications and theoretical analysis.

Herein, a commercially available and low-cost copper foam was utilized as both the catalyst for the graphdiyne synthesis and the robust 3D substrate to support the nanostructures. By a simple and mild in situ Glaser–Hay coupling reaction, ordered vertical honeycomb-like nanosize graphdiyne was created throughout the whole surface of 3D copper skeletons, providing the nanolevel structure. Combining with inherent microlevel pores of foams, a micro/nano two-tier structure was successfully constructed to provide high surface roughness. After a simple poly(dimethylsiloxane) (PDMS) coating process, the as-prepared foam showed not only extraordinary superhydrophobicity both in air (≈160.1°) and in oil (≈171.0°), but also high resistance toward abrasion cycles. Based on these features, it showed excellent performance in oil/water separation, promising for water remediation.

The overall fabrication process of graphdiyne-based superhydrophobic foam is illustrated in **Figure 1**a, mainly including two steps. First, graphdiyne was directly synthesized on the copper foam via Glaser–Hay coupling reaction. The copper foam served as both the robust and porous 3D substrate to support the nanolevel structures and the catalyst to initiate polymerization. Hexakisbenzene (HEB) served as precursor for the synthesis of graphdiyne. The catalyst distribution and precursor concentration were well controlled in the process of the Glaser–Hay coupling reaction to obtain the ordered microstructures. As a result, ordered vertical honeycomb-like nanolevel structures based on graphdiyne were grown on the copper foam. In this way, a micro/nano two-tier structure was successfully constructed providing high surface roughness. Subsequently, the graphdiyne-grown copper foam (GDCF) was covered with low-surface-energy PDMS coating by a simple vapor deposition process described elsewhere,[31] yielding a robust superhydrophobic foam (denoted as PGDCF).

Scanning electron microscopy (SEM) was used to investigate the morphology information. The copper foam has a 3D porous structure with the pore size of ≈200 μm and displays approximately the same microlevel structures (Figure 1b–d) during the overall fabrication process. The successful preparation of graphdiyne was evidenced from the Raman spectra in **Figure 2**a. Four prominent peaks around 1389.8, 1576.1, 1932.6, and 2175.1 cm^{-1} are consistent with the results previously reported.[30,32] The peak at 2175.1 cm^{-1} can be attributed to the vibration of conjugated diyne links, indicating successful coupling reaction. After graphdiyne synthesis, it is clearly observed that the smooth copper foam skeletons (Figure 1e) are covered

X. Gao, J. Zhou, R. Du, Z. Xie, Dr. S. Deng, R. Liu, Prof. Z. Liu, Prof. J. Zhang
Center for Nanochemistry
Beijing Science and Engineering Center for Nanocarbons
Beijing National Laboratory for Molecular Sciences (BNLMS)
College of Chemistry and Molecular Engineering
Peking University
Beijing 100871, P. R. China
E-mail: zfliu@pku.edu.cn; jinzhang@pku.edu.cn
J. Zhou, R. Liu
Academy for Advanced Interdisciplinary Studies
Peking University
Beijing 100871, P. R. China

DOI: 10.1002/adma.201504407

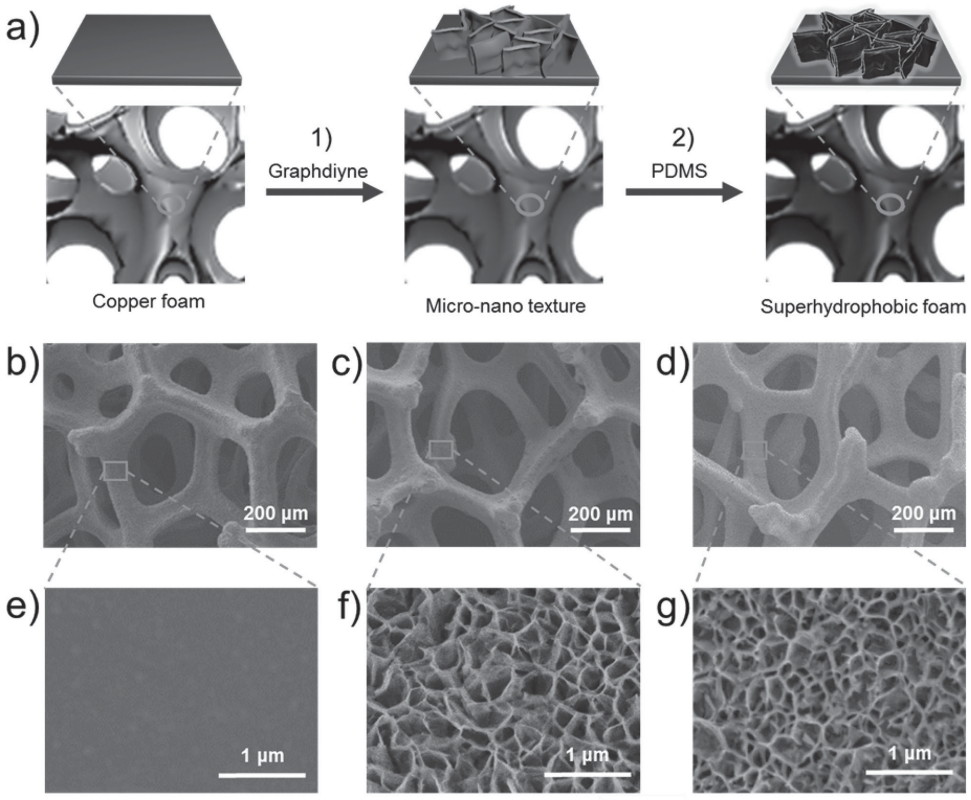

Figure 1. Fabrication process of graphdiyne-based superhydrophobic foam. a) Schematic illustration, including: 1) graphdiyne was synthesized on copper foam using a modified Glaser–Hay coupling; 2) PDMS coated the entire surface of the graphdiyne-based hierarchical structure via a vapor deposition technique. Typical SEM images of: b,e) the pure copper foam, c,f) the graphdiyne-grown copper foam, and d,g) the PDMS-modified graphdiyne-grown copper foam.

with ordered honeycomb-like graphdiyne (Figure 1f). In this way, a micro/nano hierarchical porous texture was successfully created. Furthermore, several close-up images of copper skeletons in Figure S1 (Supporting Information) show ordered nanostructures uniformly possessing the entire interconnected 3D scaffolds of copper, with an average pore size of 150 nm. The cross section (Figure S2, Supporting Information) view suggests that the honeycomb-like graphdiyne constituted of vertical

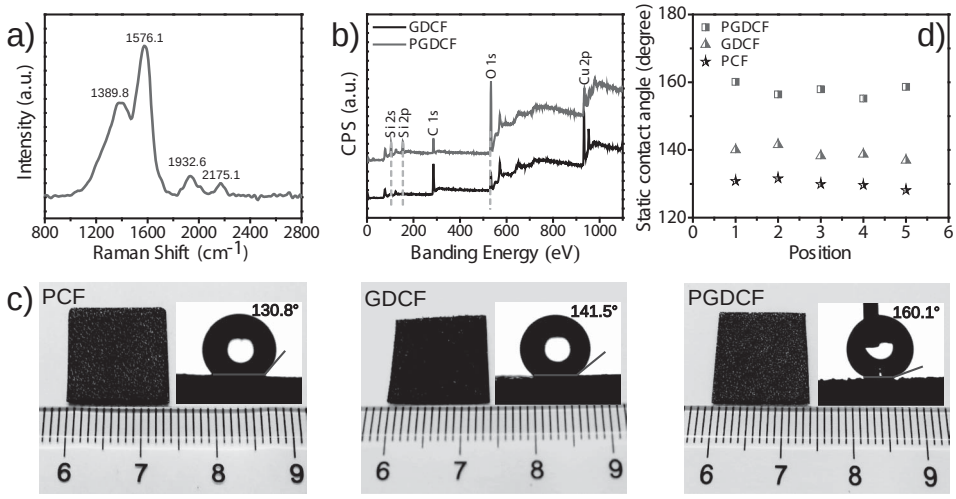

Figure 2. Characterization of as-prepared foams. a) Raman spectra of GDCF. b) XPS spectra of GDCF before and after coating with PDMS. c) Optical images of water droplets on different modified copper foams. The static contact angle (CA) of PDMS coated copper foam (PCF) is 130.8°; the static CA of graphdiyne-grown copper foam (GDCF) is 141.5°; the static CA of PDMS coated GDY-foam hierarchical texture (PGDCF) is 160.1°, exhibiting superhydrophilicity. d) Water CAs were measured at multiple points to give an average value which is representative of the entire surface; square, triangle, and star show the water CAs of PGDCF, GDCF, and PCF, respectively.

walls is ≈200 nm high. The introduction of PDMS during vapor modification can be evidenced from the appearance of silicon element in PGDCF in X-ray photoelectron spectra (XPS) (Figure 2b). Figure 1g shows that the copper foam skeletons are wrapped by a composite coating where ordered honeycomb-like graphdiyne are embedded in the PDMS matrix.

It was believed that for a rough foam, an intermediate state between Wenzel's and Cassie's states was always presented, where the droplet penetrates to some extent into the pores leaving air pockets below, as shown in Figure S3 (Supporting Information). On this condition, the contact angle can be expressed by following equation:[33]

$$\cos\theta^* = f\left(R_f \cos\theta + 1\right) - 1 \quad (1)$$

where θ^* is the static water CA, f is the apparent area fraction of solid–liquid interface, R_f is a factor of surface roughness which is defined as the ratio of the actual area of roughness surface to the geometric projected area, and θ is the water CA of a flat surface with the same material. Obviously, the optimization of the geometric structures (R_f) and the chemical compositions (θ) are two crucial pathways that can be directly controlled to improve the surface wettability of samples. For the first term, the R_f can be significantly enhanced by hierarchical microstructures in our system. Thanks to the ordered structures, the theoretical model can be easily established for surface roughness calculation (Figure S4, Supporting Information), where the graphdiyne-based nanolevel structures were modeled as a series of vertical-aligned hollow cylinders packing in a hexagonal close-packed style on the copper foam surface. In this way, a surface roughness (5.25) much higher than the pure microlevel porous foam (e.g., R_f = 2.5 in as-prepared graphene foam[17] has been acquired. Combining with inherent microlevel pores of foams, the surfaces with micro/nano porous structures which can preserve air will also make a great contribution to the factor of f. On the other hand, hydrophobicity can be predicted to be further improved via a low-surface-energy PDMS coating owing to its higher θ compared with carbon (PDMS as ≈108° and carbon as ≈86°[17]). In this way, graphdiyne-based foam coated by PDMS was expected to exhibit the best superhydrophobic behavior.

Experimentally, static contact angles (CAs) were first measured to evaluate the hydrophobic performance of different samples (Figure 2c). For PCF, the copper foam skeletons were only covered with a smooth PDMS film (similar morphology to the original copper foam) and showed a lower water CA of ≈130.8°, which proved that ordered vertical honeycomb-like nanostructures based on graphdiyne may play a vital role in the fabrication of the superhydrophobic foam. In contrast, the GDCF exhibited much higher water CA of ≈141.5°. It can be attributed to the roughness and the air pockets induced by 3D honeycomb-like graphdiyne and porous copper foam. The optical image (Figure 2c, right) shows a water droplet deposited on the PGDCF formed an almost perfect sphere and the water CA of PGDCF is ≈160.1°, which means that the surface wettability of GDCF transformed from hydrophobicity to superhydrophobicity because of low-surface-energy PDMS modification. Moreover, the as-prepared foam can maintain its superhydrophobicity (>150°) after storing in air for 3 months.

Dynamic hydrophobic performance was also assessed by advancing/receding (A/R) and sliding angle. As shown in **Figure 3**a, $\theta_{Adv}/\theta_{Rec}$ is 154.6°/98.7° which shows a high CA hysteresis (≈55.9°) and high adhesion. It could be contributed to typically two-level porosity and low carbon hydrophobicity, which can cause pinning of the water droplet front particularly during the receding of the droplet.[17] After low-surface-energy PDMS coating modification, Figure 3b shows that the advancing CA and receding CA of PGDCF are ≈161.2° and ≈153.9°. The PGDCF exhibited slight CA hysteresis (≈7.3°) and low adhesion. It can be easily understood from Equation (1) that a PDMS coating with a higher θ (≈108°) results in a higher water CA (θ^*) and thus more repellence was induced by air pockets (low f). The water droplets can be pumped easily due to these air pockets between water droplets and substrates. The low water adhesion of PGDCF was further supported by water roll-off experiments, where a sliding angle of ≈8° is obtained, much smaller than that of PF and GDCF (>40°, Figure S5b, Supporting Information). Additionally, the water droplet (≈5 µL) could quickly roll off from the surface (about 0.20 s) when PGDCF was tilted by 5° (Figure S5a, Supporting Information). Moreover, the effect of supporting substrate was investigated by replacing the 3D copper foam with 2D copper mesh (PGDCM) or copper foil (PGDCP) (see Figure S6 in the Supporting Information). It turned out that copper foam exhibited significant advantages in surface wettability, which was attributed to its typical 3D porous structure and numerous superhydrophobic surfaces.

Water droplets impinging such a surface of high water repellence and low water adhesion tended to bounce instead of being pinned. Ultrahigh speed video capture was used to monitor the interaction of water droplets with the surface of PGDCF. As shown in Figure 3c, a water droplet impinged on the PGDCF with a velocity up to 77 cm s^{-1}. As a result, the drop could bounce three times before resting on the surface. In contrast, the droplet of n-hexane could quickly spread and was then completely sucked into the PGDCF within ≈19.9 ms (Figure 3d), suggesting superoleophilicity (evidenced by an oil CA = 0°).

Abrasion resistance is another important index to evaluate the value of superhydrophobic materials for practical applications.[34] Herein, copper foam, which not only has enough high mechanical strength but also numerous replaceable surfaces along the z-direction,[13] providing a good choice for a robust supporting substrate for superhydrophobic materials. As shown in **Figure 4**a,b and Figure S7 (Supporting Information), the sandpaper abrasion test was adopted to evaluate the abrasion resistance of several substrates, including PGDCF, PGDCM, and PGDCP.

The water CAs after every abrasion cycle are shown in Figure 4c. Compared to PGDCM and PGDCP, PGDCF shows the highest robustness attributed to its typical interconnected 3D scaffold of copper foam. Further analysis established that the water CAs of PGDCF decreased from ≈157.6° to ≈147.7° after 5th cycle abrasion, but there was no obvious decreasing tendency in the subsequent multiple abrasion cycles. For further explanation, the images after 40th cycle abrasion were shown in Figure S8 (Supporting Information). The coating on the surface of copper foam was not sufficiently robust to completely resist cycle abrasion. Part of the honeycomb-like texture

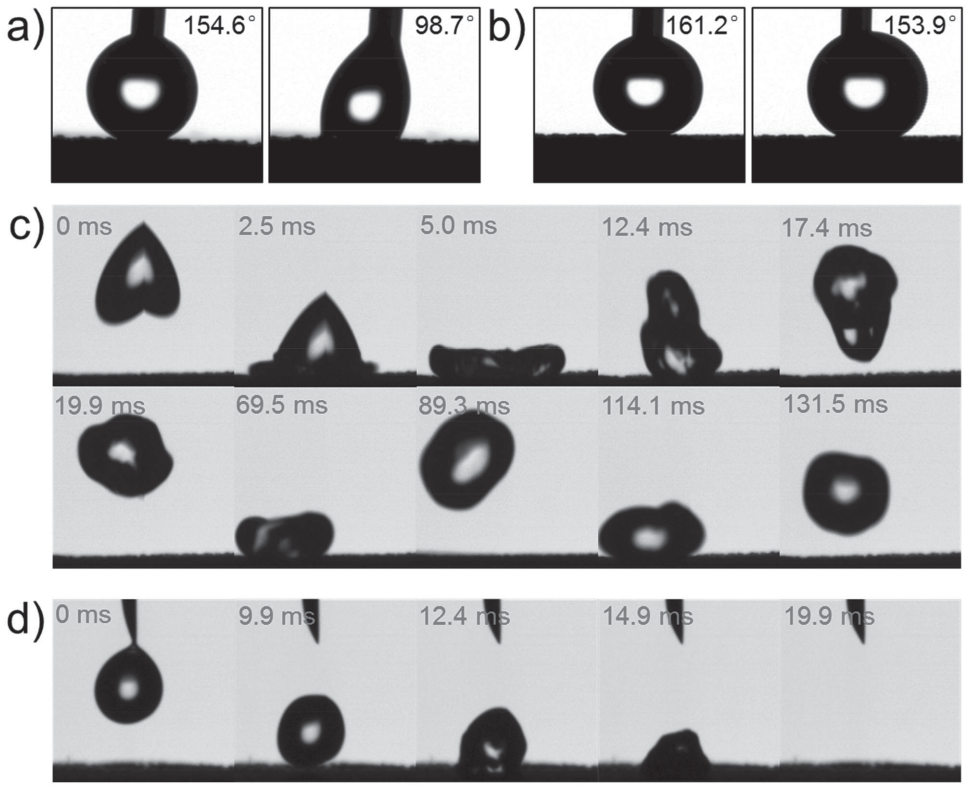

Figure 3. Measurements of foams with superwettability. a) Right: advancing liquid front for the GDCF sample indicating an advancing water CA of ≈154.6°. Lift: Receding liquid front on the same sample indicating a receding water CA of ≈98.7°. b) Corresponding advancing and receding CA on the PGDCF sample measured to be ≈161.2° and 153.9°. c) Time-lapse images of a water droplet bouncing on the PGDCF surface. Droplet sizes: ≈6.7 ± 0.2 µL. The impact velocity just prior to the droplet striking the surface was ≈77 cm s^{-1}. d) Time-lapse images of a hexane droplet sinking in the PGDCF surface.

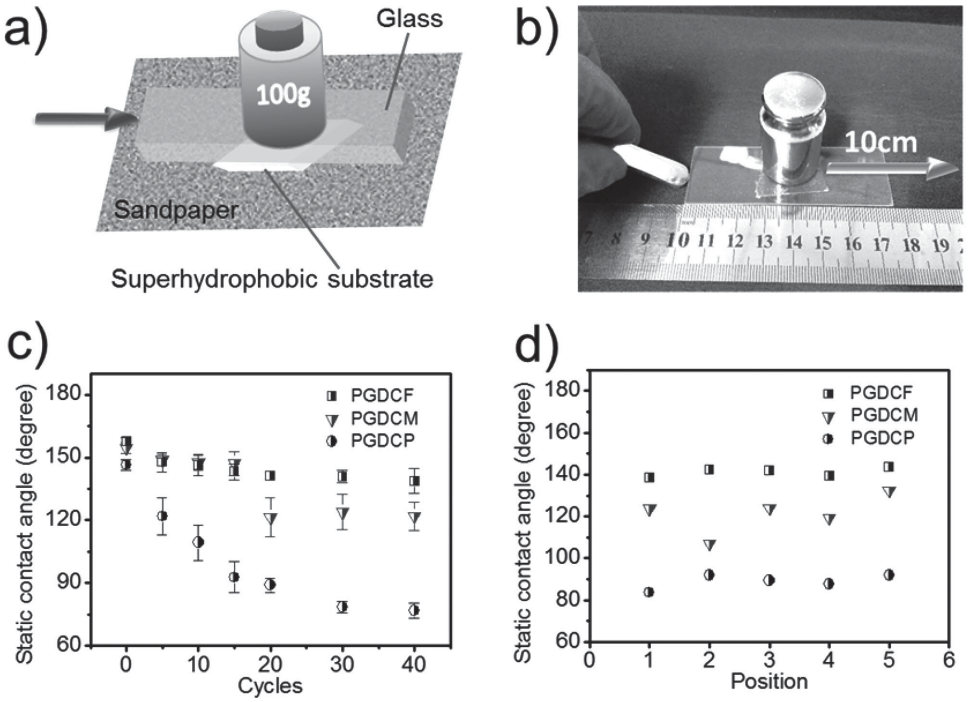

Figure 4. Mechanical resistance of PDMS/graphdiyne modified different substrates (copper foam, copper mesh, and copper foil) quantified by sandpaper abrasion tests. a) Schematic drawing of a sandpaper abrasion test. b) Process of the sandpaper abrasion cycle. c) Plot of sandpaper abrasion cycles and water CAs (measured at five different positions, taking the average) after every abrasion test. d) Water CAs taken from several positions after 20th cycle abrasion.

was eroded (Figure S8a, Supporting Information), which caused a decrease of the water CA. However, for a 3D structure, the layer beneath the top layer was well protected without any loss of superhydrophobicity, thus the material can still maintain good hydrophobicity even after many abrasion cycles (Figure S8d, Supporting Information). For PGDCP (Figure 4c, circular data points), a flat hard substrate, the nanostructures are easily destroyed (Figure S8c and S8f, Supporting Information), thus the water CAs showed an obvious decreasing tendency during the sandpaper test (from ≈146.4° to 76.8°). Furthermore, after 20th cycle abrasion we could find an obvious decrease of the water CAs PGDCP (reduced to ≈121.3°), but an average water CA of PGDCF remained more than 140° (Figure 4d). Meanwhile, SEM and optical images provide further evidence of high mechanical strength of copper foam. As shown in Figure S8a and S8b (Supporting Information), copper mesh was worn out after abrasion. But there is no visible damage in the internal space of copper foam during the sandpaper test.

More importantly, PGDCF exhibited improved superhydrophobicity in oils either lighter (*n*-hexane) or heavier (dichloromethane) than water (**Figure 5**c). A static water CA under *n*-hexane is ≈171.0°, and under dichloromethane is ≈167.2°. It can be easily understood that when it was subjected to oil/water mixture, hierarchical structures of PGDCF could trap oils and form a composite interface (oil is also highly hydrophobic) to replace original PDMS coating, thus remaining superhydrophobicity that was required in oil/water separation. Optical images (Figure 5a,b) show the dichloromethane/water separation process using the as-prepared foam (PGDCF) as separation membrane (water was labeled by orange with xylenol orange). It can be observed that when subjected to the oil/water mixture, the PGDCF can selectively block the water and allowed oil to pass by, with a high separation efficiency (>98%) estimated by previous method.[35] The separation mechanism was based on the superhydrophobicity and superoleophilicity of PGDCF. Owing to the existence of large microsize pores and excellent water repellency, the PGDCF allowed oils to quickly pass through the pores by gravity while the water would remained on the surface by the high water repulsive forces. Based on this mechanism, after use, the device can be regenerated easily by cleaning with the appropriate solvent (e.g., ethanol) for exhibiting good recyclability.

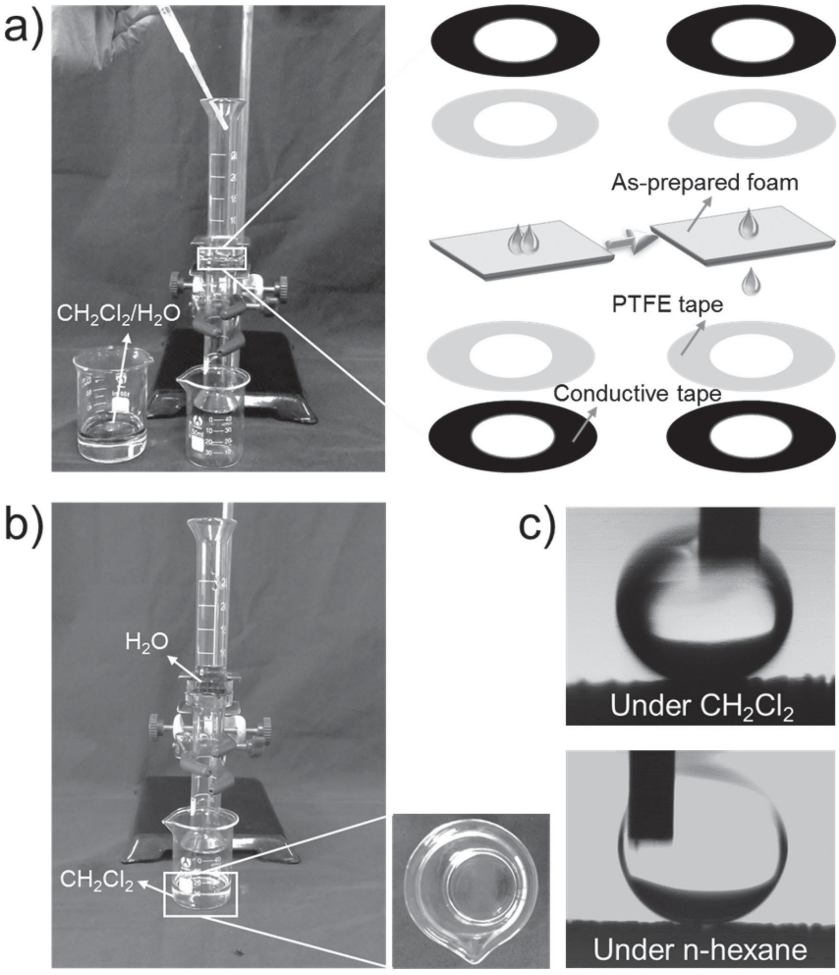

Figure 5. Oil/water separation test and its mechanism. a) Separation apparatus with a dichloromethane/water mixture above as-prepared foam (PGDCF). Conductive tape and polytetrafluoroethylene (PTFE) tape were fixed on glass tubes, sequentially, and then PGDCF sandwiched between the two glass tubes. b) Dichloromethane passed through PGDCF whereas water (labeled by orange with xylenol orange) was retained. c) The photograph of water droplet on the PGDCF surface under oil. CA water (dichloromethane) ≈167.2°; CA water (*n*-hexane) ≈171.0°.

To further study the separation ability of the as-prepared foam, we measured the intrusion pressure of water flowing through the foam, which indicates the maximum height of water that the PGDCF can support. The intrusion pressure is provided by the weight of water, therefore, the intrusion pressure (p) values were calculated using equation:

$$p = \rho g h_{max} \quad (2)$$

where ρ is the density of the water, g is acceleration of gravity, and h_{max} is the maximum height of water PGDCF can support. The intrusion pressures for water in our system were about 0.87 kPa. It means that water cannot flow through the foam below the intrusion pressure.

In summary, an ingenious design to fabricate a uniform layer of graphdiyne-based ordered nanostructures (nanometer-level roughness) on copper foam (micrometer-level roughness) via in situ Glaser–Hay coupling by using copper foam as both robust 3D porous substrate and catalyst is presented. Coupled with PDMS coating, the resultant PGDCF exhibited superior superhydrophobicity with high water CA (≈160°), small CA hysteresis (≈7.3°), and low sliding angle (≈8°), in agreement with its high

surface roughness (≈5.25) calculated by theoretical modeling. Moreover, the deliberately selected copper foam also endows the PGDCF with high abrasion resistance, thus simultaneously integrating superhydrophobicity and high mechanical strength in one material, important for practical applications. Additionally, as one example, PGDCF was used for oil/water separation, exhibiting both high efficiency and good recyclability. The as-presented design may open a new window for designing robust superhydrophobic materials for water remediation. Additionally, considering the intrinsic unique physicochemical properties of graphdiyne, this graphdiyne-based foam may also show great potential in various fields such as energy storage and sensors.

Experimental Section

Preparation of GDCF: Pretreated-copper foam was immersed in the mixed solution of TMEDA, pyridine, and acetone, and then the solution of HEB was added dropwise. The mixture was heated under an argon atmosphere at 50 °C for 12 h. Ordered vertical honeycomb-like graphdiyne were synthesized on the copper foam. This graphdiyne-grown copper foam was washed with heated acetone and *N*,*N*-dimethylformamide (DMF), sequentially, to remove monomers and oligomers, and then dried under a flow of nitrogen. Finally, GDCF was obtained by this protocol.

Preparation of PGDCF: We coated GDCF using PDMS by a vapor deposition technique.[31] In detail, we placed the as-prepared GDCF into a glass container which covered with a PDMS film, and then the glass container was kept at 235 °C for 8 h.

Supporting Information

Supporting Information is available from the Wiley Online Library or from the author.

Acknowledgements

This work was supported by the NSFC (Grant Nos. 51432002, 21233001, 21129001, 51272006, and 51121091).

Received: September 8, 2015
Revised: September 22, 2015
Published online: November 9, 2015

[1] R. Blossey, *Nat. Mater.* **2003**, *2*, 301.
[2] X. Deng, L. Mammen, H. J. Butt, D. Vollmer, *Science* **2012**, *335*, 67.
[3] X. F. Gao, X. Yan, X. Yao, L. Xu, K. Zhang, J. H. Zhang, B. Yang, L. Jiang, *Adv. Mater.* **2007**, *19*, 2213.
[4] Z. Q. Sun, T. Liao, K. S. Liu, L. Jiang, J. H. Kim, S. X. Dou, *Small* **2014**, *10*, 3001.
[5] L. Yao, J. He, *Chin. J. Chem.* **2014**, *32*, 507.
[6] F. Zhang, W. B. Zhang, Z. Shi, D. Wang, J. Jin, L. Jiang, *Adv. Mater.* **2013**, *25*, 4192.
[7] C. R. Crick, J. A. Gibbins, I. P. Parkin, *J. Mater. Chem. A* **2013**, *1*, 5943.
[8] X. Hou, Y. H. Hu, A. Grinthal, M. Khan, J. Aizenberg, *Nature* **2015**, *519*, 70.
[9] J. Zhu, C. M. Hsu, Z. Yu, S. Fan, Y. Cui, *Nano Lett.* **2010**, *10*, 1979.
[10] W. Barthlott, C. Neinhuis, *Planta* **1997**, *202*, 1.
[11] L. Feng, S. H. Li, Y. S. Li, H. J. Li, L. J. Zhang, J. Zhai, Y. L. Song, B. Q. Liu, L. Jiang, D. B. Zhu, *Adv. Mater.* **2002**, *14*, 1857.
[12] S. T. Wang, K. S. Liu, X. Yao, L. Jiang, *Chem. Rev.* **2015**, *115*, 8230.
[13] D. M. Zang, C. X. Wu, R. W. Zhu, W. Zhang, X. Q. Yu, Y. F. Zhang, *Chem. Commun.* **2013**, *49*, 8410.
[14] Y. Lin, G. J. Ehlert, C. Bukowsky, H. A. Sodano, *ACS Appl. Mater. Interfaces* **2011**, *3*, 2200.
[15] Y. Si, Q. Fu, X. Wang, J. Zhu, J. Yu, G. Sun, B. Ding, *ACS Nano* **2015**, *9*, 3791.
[16] X. C. Dong, J. Chen, Y. W. Ma, J. Wang, M. B. Chan-Park, X. M. Liu, L. H. Wang, W. Huang, P. Chen, *Chem. Commun.* **2012**, *48*, 10660.
[17] E. Singh, Z. Chen, F. Houshmand, W. Ren, Y. Peles, H. M. Cheng, N. Koratkar, *Small* **2013**, *9*, 75.
[18] D. D. Nguyen, N. H. Tai, S. B. Lee, W. S. Kuo, *Energy Environ. Sci.* **2012**, *5*, 7908.
[19] H. Zhu, D. Chen, W. An, N. Li, Q. Xu, H. Li, J. He, J. Lu, *Small* **2015**, DOI: 10.1002/smll.201501004.
[20] C. P. Ruan, K. L. Ai, X. B. Li, L. H. Lu, *Angew. Chem. Int. Ed.* **2014**, *53*, 5556.
[21] J. Xu, J. L. Xu, Y. Cao, X. B. Ji, Y. Y. Yan, *Appl. Surf. Sci.* **2013**, *286*, 220.
[22] R. Gao, Q. Liu, J. Wang, J. Y. Liu, W. L. Yang, Z. Gao, L. H. Liu, *Appl. Surf. Sci.* **2014**, *289*, 417.
[23] C. S. Huang, S. L. Zhang, H. B. Liu, Y. G. Li, G. L. Cui, Y. L. Li, *Nano Energy* **2015**, *11*, 481.
[24] H. Y. Zhang, Y. Y. Xia, H. X. Bu, X. P. Wang, M. Zhang, Y. H. Luo, M. W. Zhao, *J. Appl. Phys.* **2013**, *113*, 044309.
[25] J. Y. Xiao, J. J. Shi, H. B. Liu, Y. Z. Xu, S. T. Lv, Y. H. Luo, D. M. Li, Q. B. Meng, Y. L. Li, *Adv. Energy Mater.* **2015**, *5*, 1401943.
[26] H. T. Qi, P. Yu, Y. X. Wang, G. C. Han, H. B. Liu, Y. P. Yi, Y. L. Li, L. Q. Mao, *J. Am. Chem. Soc.* **2015**, *137*, 5260.
[27] X. Zhang, M. S. Zhu, P. L. Chen, Y. J. Li, H. B. Liu, Y. L. Li, M. H. Liu, *Phys. Chem. Chem. Phys.* **2015**, *17*, 1217.
[28] S. Wang, L. Yi, J. E. Halpert, X. Lai, Y. Liu, H. Cao, R. Yu, D. Wang, Y. Li, *Small* **2012**, *8*, 265.
[29] G. X. Li, Y. L. Li, X. M. Qian, H. B. Liu, H. W. Lin, N. Chen, Y. J. Li, *J. Phys. Chem. C* **2011**, *115*, 2611.
[30] J. Y. Zhou, X. Gao, R. Liu, Z. Q. Xie, J. Y. Yang, S. Q. Zhang, G. M. Zhang, H. B. Liu, Y. L. Li, J. Zhang, Z. F. Liu, *J. Am. Chem. Soc.* **2015**, *137*, 7596.
[31] J. K. Yuan, X. G. Liu, O. Akbulut, J. Q. Hu, S. L. Suib, J. Kong, F. Stellacci, *Nat. Nanotechnol.* **2008**, *3*, 332.
[32] G. X. Li, Y. L. Li, H. B. Liu, Y. B. Guo, Y. J. Li, D. B. Zhu, *Chem. Commun.* **2010**, *46*, 3256.
[33] A. Marmur, *Langmuir* **2003**, *19*, 8343.
[34] Y. Lu, S. Sathasivam, J. L. Song, C. R. Crick, C. J. Carmalt, I. P. Parkin, *Science* **2015**, *347*, 1132.
[35] X. Y. Zhang, Z. Li, K. S. Liu, L. Jiang, *Adv. Funct. Mater.* **2013**, *23*, 2881.